Digital RAC for Underwater Vehicle-Manipulator Systems Considering Singular Configuration

Shinichi Sagara Masakazu Tamura Takashi Yatoh Kenzo Shibuya
Department of Control Engineering, Kyushu Institute of Technology
Tobata, Kitakyushu 804-8550, Japan
E-mail: sagara@cntl.kyutech.ac.jp

Abstract

We have proposed continuous-time and discrete-time resolved acceleration control methods for underwater vehicle-manipulator systems and the effectiveness of the control methods have been shown by experiments. In this paper, we propose a digital control method considering singular configuration of manipulator. Experimental result shows the effectiveness of the proposed method.

1 Introduction

Underwater robots, especially Underwater Vehicle-Manipulator Systems (UVMS), are expected to make important roles in ocean exploration. Many studies about dynamics and control of UVMS have been reported [1–3], however the experimental studies are only a few.

We have proposed continuous-time and discrete-time Resolved Acceleration Control (RAC) methods for UVMS [4–6], and the effectiveness of the RAC methods are demonstrated by using a floating underwater robot with vertical planar 2-link manipulator shown in Fig. 1. There is no discrete-time control method for UVMS except our proposed method. The performances of both control methods are similar, however position and velocity feedback gains of the discrete version cannot set separately. So we have proposed a new discrete-time RAC method whose feedback gains can set individually [7].

Here, in the case of singular configuration of manipulators the control input cannot be generally calculated. So, in this paper, we propose a discrete-time RAC method considering singular configuration of manipulator. To keep away from singular configuration, desired position of the vehicle is modified based on the determinant of the manipulator's Jacobian matrix. The effectiveness of the proposed method is shown by experiment.

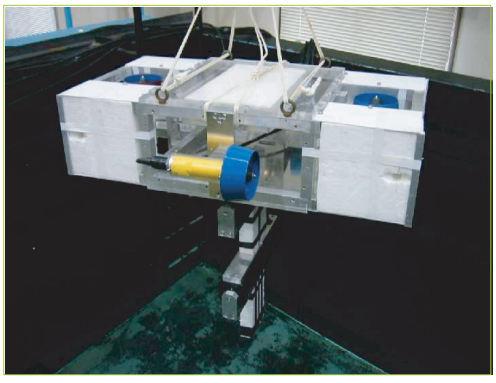

Fig. 1 Floating 2-link underwater robot

2 Modeling [4]

The underwater robot model used in this paper is shown in Fig. 2. It has a robot base (vehicle) and

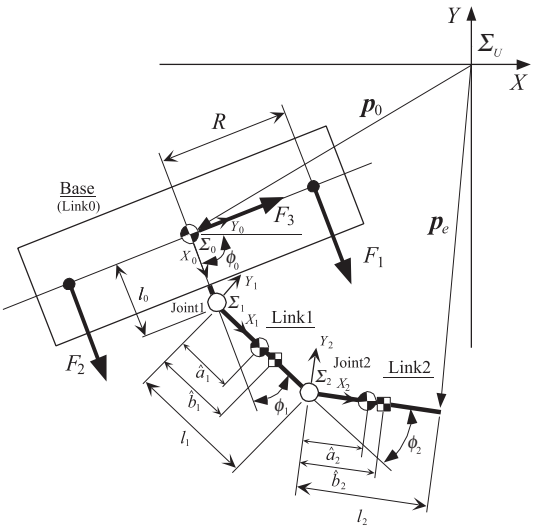

Fig. 2 2-link underwater robot model

2-DOF manipulator that can move in a vertical plane. Thrusters are mounted on the base to provide propulsion for position and attitude control of the base. Symbols used in Fig. 2 as follows:

- Σ_U : inertial coordinate frame
- Σ_i : ith link coordinate frame ($i = 0,\ 1,\ 2$; link 0 means base)
- l_i : length of link i
- ϕ_i : relative joint angle
- $\boldsymbol{p}_0$: position vector of origin of Σ_0 with respect to Σ_U
- $\boldsymbol{p}_e$: position vector of end-tip of manipulator with respect to Σ_U
- $\hat{\boldsymbol{a}}_i$: position vector from joint i to center of gravity of link i with respect to Σ_i
- $\hat{\boldsymbol{b}}_i$: position vector from joint i to center of buoyancy of link i with respect to Σ_i
- F_j : thruster force ($j = 1,\ 2,\ 3$)
- R : length form origin of Σ_0 to thruster

First, from Fig. 2 a time derivative of $\boldsymbol{p}_e$ is

$$\dot{\boldsymbol{p}}_e = \boldsymbol{A}\dot{\boldsymbol{x}}_0 + \boldsymbol{B}\dot{\boldsymbol{\phi}} \tag{1}$$

where $\boldsymbol{x}_0 = [\boldsymbol{p}_0^T,\ \phi_0]^T$ and $\boldsymbol{\phi} = [\phi_1,\ \phi_2]^T$, $\boldsymbol{A} \in R^{2\times 3}$ and $\boldsymbol{B} \in R^{2\times 2}$ are matrices consisting of attitude angle of base and joint angles.

Next, let $\boldsymbol{\eta}$ and $\boldsymbol{\mu}$ be a linear and an angular momentum of the robot including hydrodynamic added mass tensor $\boldsymbol{M}_{a_i}$ and added inertia tensor $\boldsymbol{I}_{a_i}$ of link i. Then

$$\boldsymbol{\eta} = [\eta_1,\ \eta_2,\ 0]^T = \sum_{i=0}^{2} \boldsymbol{N}_i, \tag{2}$$

$$\boldsymbol{\mu} = [0,\ 0,\ \mu_3]^T = \sum_{i=0}^{2} (\boldsymbol{I}_i + \boldsymbol{I}_{a_i})\boldsymbol{\omega}_i + \hat{\boldsymbol{x}}_i \times \boldsymbol{N}_i \tag{3}$$

where $\boldsymbol{N}_i = {}^U\boldsymbol{R}_i(m_i\boldsymbol{E} + \boldsymbol{M}_{a_i})\tilde{\boldsymbol{a}}_i$ and m_i is the mass of link i, ${}^U\boldsymbol{R}_i$ is the coordinate transformation matrix from Σ_i to Σ_U, $\boldsymbol{I}_i$ is the inertia tensor of link i, $\boldsymbol{E}$ is the unit matrix, $\tilde{\boldsymbol{a}}_i = \boldsymbol{v}_i + \boldsymbol{\omega}_i \times \hat{\boldsymbol{a}}_i$, $\boldsymbol{v}_i$ is the velocity vector of link i with respect to Σ_i, $\boldsymbol{\omega}_i = [0,\ 0,\ \dot{\phi}_i]^T$.

From Eqs. (1)-(3) the following equation can be obtained:

$$\boldsymbol{s} = [\eta_1,\ \eta_2,\ \mu_3]^T = \boldsymbol{C}\dot{\boldsymbol{x}}_0 + \boldsymbol{D}\dot{\boldsymbol{\phi}} \tag{4}$$

where $\boldsymbol{C} \in R^{3\times 3}$ and $\boldsymbol{D} \in R^{3\times 2}$ are matrices including the added mass $\boldsymbol{M}_{a_i}$ and the added inertia $\boldsymbol{I}_{a_i}$.

In the meanwhile, the drag force and moment of joint i can be generally represented as follows [8,9]:

$$\boldsymbol{f}_{d_i} = \frac{\rho}{2} C_{D_i} D_i \int_0^{l_i} ||\boldsymbol{w}_i|| \boldsymbol{w}_i d\hat{\boldsymbol{x}}_i, \tag{5}$$

$$t_{d_i} = \frac{\rho}{2} C_{D_i} D_i \int_0^{l_i} \hat{\boldsymbol{x}}_i ||\boldsymbol{w}_i|| \boldsymbol{w}_i d\hat{\boldsymbol{x}}_i \tag{6}$$

where $\boldsymbol{w}_i = \boldsymbol{v}_i + \boldsymbol{\omega}_i \times \hat{\boldsymbol{x}}_i$, and ρ is the fluid density, C_{D_i} is the drag coefficient, D_i is the width of link i.

Furthermore, the gravitational and buoyant forces acting link i are described as follows:

$$\boldsymbol{f}_{g_i} = ({}^U\boldsymbol{R}_i)^T(\rho V_i - m_i)\boldsymbol{g}, \tag{7}$$

$$\boldsymbol{t}_{g_i} = ({}^U\boldsymbol{R}_i)^T(\hat{\boldsymbol{b}}_i \times \rho V_i \boldsymbol{g} - \hat{\boldsymbol{a}}_i \times m_i \boldsymbol{g}) \tag{8}$$

where V_i is the volume of link i and $\boldsymbol{g}$ is the gravitational acceleration vector.

3 Control method

In this section, we propose a control method of UVMS considering singular configuration of manipulator.

3.1 Digital RAC [7]

Differentiating Eqs. (1) and (4) with respect to time, the following equation can be obtained:

$$\boldsymbol{W}(t)\boldsymbol{\alpha}(t) = \beta(t) + \boldsymbol{f}(t) - \dot{\boldsymbol{W}}(t)\boldsymbol{v}(t) \tag{9}$$

where

$$\boldsymbol{W} = \begin{bmatrix} \boldsymbol{C}+\boldsymbol{E} & \boldsymbol{D} \\ \boldsymbol{A} & \boldsymbol{B} \end{bmatrix}, \quad \boldsymbol{\alpha} = \begin{bmatrix} \ddot{\boldsymbol{x}}_0 \\ \ddot{\boldsymbol{\phi}} \end{bmatrix},$$

$$\beta = \begin{bmatrix} \ddot{\boldsymbol{x}}_0 \\ \ddot{\boldsymbol{p}}_e \end{bmatrix}, \quad \boldsymbol{f} = \begin{bmatrix} \boldsymbol{s} \\ \boldsymbol{0} \end{bmatrix}, \quad \boldsymbol{v} = \begin{bmatrix} \dot{\boldsymbol{x}}_0 \\ \dot{\boldsymbol{\phi}} \end{bmatrix}$$

and $\boldsymbol{s}$ is the external force including hydrodynamic force and thrust of the thruster which act on the robot.

Discretizing Eq. (9) by a sampling period T, and applying $\beta(k)$ and $\dot{\boldsymbol{W}}(k)$ to the backward Euler approximation, we have

$$\boldsymbol{W}(k)\boldsymbol{\alpha}(k-1) = \frac{1}{T}[\boldsymbol{\nu}(k) - \boldsymbol{\nu}(k-1) + T\boldsymbol{f}(k) - \{\boldsymbol{W}(k) - \boldsymbol{W}(k-1)\}\boldsymbol{v}(k)] \tag{10}$$

where $\boldsymbol{\nu} = \left[\dot{\boldsymbol{x}}_0^T,\ \dot{\boldsymbol{p}}_e^T\right]^T$. Note that computational time delay is introduced to Eq. (10) and the discrete time kT is abbreviated to k.

For Eq. (10) the desired acceleration is defined as

$$\boldsymbol{\alpha}_d(k) = \frac{1}{T}\boldsymbol{W}^{-1}(k)[\boldsymbol{\nu}_d(k+1) - \boldsymbol{\nu}_d(k) + \boldsymbol{\Lambda}\boldsymbol{e}_\nu(k) + T\boldsymbol{f}(k)] \tag{11}$$

where

$$\boldsymbol{e}_\nu(k) = \boldsymbol{\nu}_d(k) - \boldsymbol{\nu}(k) \tag{12}$$

and $\boldsymbol{\nu}_d(k)$ is the desired value of $\boldsymbol{\nu}(k)$, $\boldsymbol{\Lambda}$=diag$\{\lambda_i\}$ $(i = 1, \cdots, 5)$ is the velocity feedback gain matrix.

From Eqs. (10) and (11) we have

$$\begin{aligned} T\boldsymbol{W}(k)\boldsymbol{e}_\alpha(k-1) = {} & \boldsymbol{e}_\nu(k) - \boldsymbol{e}_\nu(k-1) + \boldsymbol{\Lambda}\boldsymbol{e}_\nu(k) \\ & - T\{\boldsymbol{f}(k) - \boldsymbol{f}(k-1)\} \\ & + \{\boldsymbol{W}(k) - \boldsymbol{W}(k-1)\}\boldsymbol{v}(k) \end{aligned} \tag{13}$$

where $\boldsymbol{e}_\alpha(k) = \boldsymbol{\alpha}_d(k) - \boldsymbol{\alpha}(k)$. Assuming $\boldsymbol{W}(k) \approx \boldsymbol{W}(k-1)$ and $\boldsymbol{f}(k) \approx \boldsymbol{f}(k-1)$ for one sampling period, Eq. (13) can be rewritten as follows:

$$T\boldsymbol{W}(k+1)\boldsymbol{e}_\alpha(k) = \{(q-1)\boldsymbol{E} + \boldsymbol{\Lambda}\}\,\boldsymbol{e}_\nu(k) \tag{14}$$

where q is the forward sift operator. From Eq. (14), if λ_i is selected to satisfy $0< \lambda_i <1$, the convergence of $\boldsymbol{e}_\alpha(k)$ to zero as k tends to infinity and all elements of $\boldsymbol{W}(k)$ are bounded, $\boldsymbol{e}_\nu(k)\to\boldsymbol{0}$ $(k\to\infty)$ can be ensured.

Furthermore, the desired velocity is defined as

$$\boldsymbol{\nu}_d(k) = \frac{1}{T}\{\boldsymbol{p}_d(k) - \boldsymbol{p}_d(k-1) + \boldsymbol{\Gamma}\boldsymbol{e}_p(k-1)\} \tag{15}$$

where $\boldsymbol{e}_p(k) = \boldsymbol{p}_d(k) - \boldsymbol{p}(k)$ and $\boldsymbol{p}(k) = [\boldsymbol{x}_0^T(k), \boldsymbol{p}_e^T(k)]^T$, $\boldsymbol{p}_d(k)$ is the desired value of $\boldsymbol{p}(k)$, $\boldsymbol{\Gamma}$=diag$\{\gamma_i\}$ $(i=1, \cdots, 5)$ is the position feedback gain matrix.

From Eq. (12) and (15) the following equation can be obtained:

$$T\boldsymbol{e}_\nu(k) = \left\{\boldsymbol{E} - (\boldsymbol{E} - \boldsymbol{\Gamma})\,q^{-1}\right\}\boldsymbol{e}_p(k) \tag{16}$$

where $\boldsymbol{\nu}(k)$ is applied to the backward Euler approximation. From Eq. (16), if γ_i is selected to satisfy $0< \gamma_i <1$ and the convergence of $\boldsymbol{e}_\nu(k)$ to zero as k tends to infinity, $\boldsymbol{e}_p(k)\to\boldsymbol{0}$ $(k\to\infty)$ can be ensured.

3.2 Avoidance of singular configuration

In many works of UVMS it is considered that the vehicle is keeping the initial state during manipulation. Then, to keep away from singular configuration of manipulator, the desired value of vehicle is modified by using the determinant of Jacobian matrix $J(k)$=det$\boldsymbol{J}(k)$ of manipulator.

The desired linear acceleration of vehicle $\ddot{\boldsymbol{p}}_{0_d} = [\ddot{p}_{0x_d},\ \ddot{p}_{0y_d}]^T$ is defined as

$$\ddot{p}_{0*_d} = \begin{cases} \dot{p}_{e*_d}^2/|\dot{p}_{e*_d}| & (k_1 \le k < k_1 + n) \\ 0 & (\text{otherwise}) \\ -\dot{p}_{e*_d}^2/|\dot{p}_{e*_d}| & (k_2 \le k < k_2 + n) \end{cases} \tag{17}$$

where $*$ denotes x or y, and $\dot{p}_{e*_d}$ is the desired value of end-tip of manipulator, k_1T and k_2T are the time at the time when $|J(k)|$ becomes less and greater than the threshold J_s respectively, nT is the acceleration time.

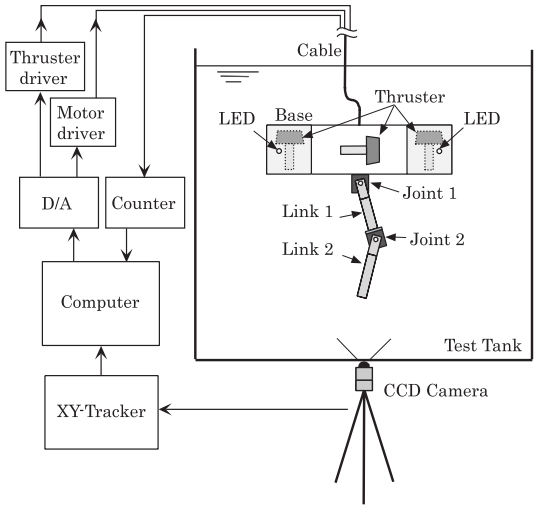

Fig. 3 Configuration of underwater robot system

Table 1 Physical parameters of underwater robot

	Base	Link 1	Link 2
Mass [kg]	26.04	4.25	1.23
Moment of inertia [kg m^2]	1.33	0.19	0.012
Link length (x axis) [m]	0.2	0.25	0.25
Link length (y axis) [m]	0.81	0.04	0.04
Link width [m]	0.42	0.12	0.12
Added mass(x) [kg]	72.7	1.31	0.1
Added mass(y) [kg]	6.28	3.57	2.83
Added moment of inertia [kg m^2]	1.05	0.11	0.06
Drag coefficient(x)	1.2	0	0
Drag coefficient(y)	1.2	1.2	1.2

4 Experiment

In this section, to verify the effectiveness of the proposed control method, the experiment is done.

Fig. 3 shows a configuration of experimental system. Physical parameters of the underwater robot are shown in Table 1. The details of the system, tne dynamic equation of robot and thruster characteristics are shown in [4].

The experiment was carried out under the following condition. The desired end-tip position was set up along a straight path from the initial position to the target. On the other hand, the basic desired position and attitude of vehicle were set up the initial values, and the threshold of the determinant of Jacobian matrix was $J_s = 0.45$. The sampling period was T=1/60[s] and the feedback gains were $\boldsymbol{\Lambda}$ = diag$\{0.6,\ 0.6,\ 0.25,\ 0.25,\ 0.25\}$ and $\boldsymbol{\Gamma}$ =

diag{0.6, 0.6, 0.2, 0.25, 0.25}. Furthermore, the initial relative angles of the robot were $\phi_0 = -\pi/2$[rad], $\phi_1 = \pi/3$[rad] and $\phi_2 = -5\pi/18$[rad].

The typical experimental result is shown in Fig. 4. From Fig. 4 it can be seen that the end-tip of manipulator and base follow the reference trajectories in spite of the influence of the hydrodynamic forces and the tracking errors are very small. The experimental result shows that the control performance can be improved by using the proposed method.

5 Conclusion

In this paper, a digital RAC system for UVMS was proposed. The experimental result showed the effectiveness of the proposed method.

References

[1] T. W. McLain *et al.*, "Experiments in the Coordinated Control of an Underwater Arm/Vehicle System", *Autonomous Robots 3*, Kluwer Academic Publishers, pp. 213 – 232, 1996.

[2] G. Antonelli *et al.*, "Tracking Control for Underwater Vehicle-Manipulator Systems with Velocity Estimation", *IEEE J. Oceanic Eng.*, Vol. 25, No. 3, pp. 399 – 413, 2000.

[3] N. Sarkar and T. K. Podder, "Coordinated Motion Planning and Control of Autonomous Underwater Vehicle-Manipulator Systems Subject to Drag Optimization", *IEEE J. Oceanic Eng.*, Vol. 26, No. 2, pp. 228 – 239, 2001.

[4] S. Yamada and S. Sagara, "Resolved Motion Rate Control of an Underwater Robot with Vertical Planar 2-Link Manipulator", *Proc. of AROB 7th*, pp. 230 – 233, 2002.

[5] S. Sagara, "Digital Control of an Underwater Robot with vertical Planar 2-Link Manipulator", *Proc. of AROB 8th*, pp. 524 – 527, 2003.

[6] S. Sagara, K. Shibuya and M. Tamura, "Experiment of Digital RAC for an Underwater Robot with vertical Planar 2-Link Manipulator", *Proc. of AROB 9th*, pp. 337 – 340, 2004.

[7] S. Sagara, K. Shibuya and M. Tamura, "Digital Resolved Acceleration Control of Underwater Vehicle-Manipulator Systems", *Proc. Int. Symp. Bio-inspired Systems*, Part V: Robotics and Motion Control, pp. 21 – 26, 2004.

[8] B. Lévesque and M. J. Richard, "Dynamic Analysis of a Manipulator in a Fluid Environment", *Int. J. Robot. Res.*, Vol. 13, No. 3, pp. 221 – 231, 1994.

[9] S. McMillan *et al.*, "Efficient Dynamic Simulation of an Underwater Vehicle with a Robotic Manipulator", *IEEE Trans. Syst., Man, Cybern.*, Vol. 25, No. 8, pp. 1194 – 1206, 1995.

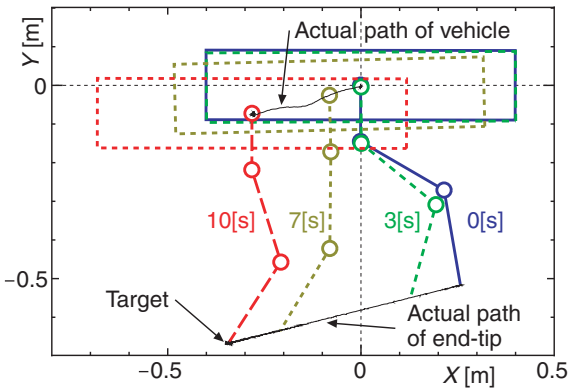

(a) motion

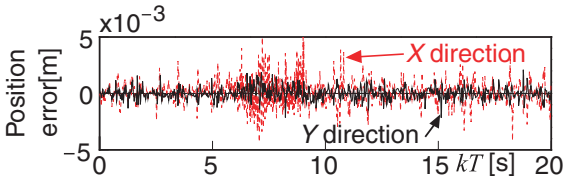

(b) position error of end-tip

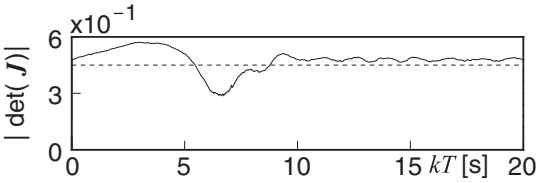

(c) determinant of J

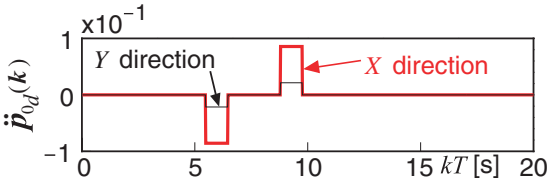

(d) desired acceleration of base position

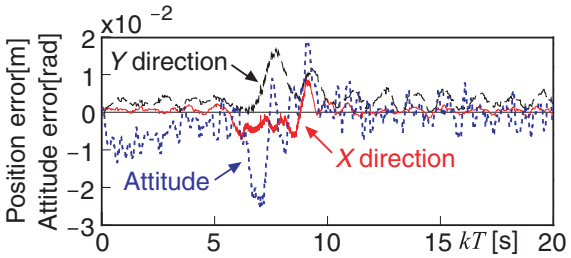

(e) position and attitude error of base

Fig. 4 Experimental result